Bolanos-Sanchez, Rodolfo; Brown, Jennifer M.; Amoudry, Laurent O.; Souza, Alejandro J.. 2013 Tidal, Riverine, and Wind Influences on the Circulation of a Macrotidal Estuary. *Journal of Physical Oceanography*, 43 (1). 29-50. 10.1175/JPO-D-11-0156.1

Tidal, Riverine, and Wind Influences on the Circulation of a Macrotidal Estuary

RODOLFO BOLAÑOS,* JENNIFER M. BROWN, LAURENT O. AMOUDRY, AND ALEJANDRO J. SOUZA

National Oceanography Centre, Liverpool, United Kingdom

(Manuscript received 2 September 2011, in final form 24 September 2012)

ABSTRACT

The effect of tides, river, wind and Earth's rotation on the three-dimensional circulation in the Dee, a macrotidal estuary, are investigated using a fine-resolution model. The interactions of the large tidal amplitude, currents, river, and wind-generated circulation require baroclinic and unsteady studies to properly understand the estuarine dynamics. Assessment of the model skill has been carried out by model–observation comparisons for salinity, which is the main control for density, surface elevation, current, and turbulence. Stationary nondimensional numbers were only partially able to characterize the dynamics in this (real) complex macrotidal estuary. At low water, tidal straining and constrained river flow cause stratification. Large spatial variability occurs in the current and residual patterns, with flood-dominated maximum values occurring within the tidal channels. The tides control residual circulation by modulating stratification through tidal straining and bathymetric constraint on river flow. Tide–stratification–river interaction causes an unsteady pattern of residual circulation and tidal pulses. River-induced pulses are enhanced near low tide–inducing density-driven circulation. Wind effects are concentrated near the surface, mainly occurring at high tide because of increased fetch. Even though Coriolis has, overall, a small contribution it produces tidal pulses modifying the current and salinity distribution.

1. Introduction

a. Circulation in estuaries

Circulation in estuaries is very complex, characterized by the interactions of tidal currents, bathymetric constraint, strong turbulence, and steep density gradients. Although tidal currents may have large velocities, the much weaker residual currents are important in determining the transport of dissolved and particulate matter in suspension. Understanding the processes that control circulation is therefore vital for long-term estuarine management. Residual estuarine circulation is generally referred to as gravitational circulation, with density gradients driving a seaward surface flow and landward near-bed flow (e.g., Pritchard 1952; Hansen and Rattray 1965). These density gradients are mainly determined by the competition between riverine buoyancy and vertical tidal mixing. However, residual circulation within estuaries can also be induced by tides, lateral advection, straining, wind, and interactions between these forcings.

Typically, tidal mixing is stronger during the flood than the ebb, creating a two-layer circulation with seaward flow near the surface and landward flow near the bottom. Tidal asymmetry in turbulent mixing, caused by strain-induced periodic stratification (Simpson et al. 1990), has been suggested to cause residual currents (Jay and Smith 1990; Stacey 2001). The relative importance of density gradients and tidal components on residual circulation depends on the particular characteristics of the estuary, such as tidal range, freshwater input, and morphology (e.g., Prandle 2009). Burchard and Hetland (2010) numerically showed that, in the absence of wind influence, the intensity of the gravitational circulation scales with the horizontal Richardson numbers (also referred to as the Simpson number) over a wide range of values. They found it is about one-third of the total estuarine circulation, while the other two thirds are due to tidal straining, which is also dependent on the Richardson number and weakly dependent on the Strouhal number. The tidally strained contribution to the residual profile has similar shape to that of the gravitational circulation;

* Current affiliation: DHI, Hørsholm, Denmark.

Corresponding author address: Rodolfo Bolaños, DHI, Agern Allé 5, DK-2970 Hørsholm, Denmark.
E-mail: rbol@dhigroup.com

DOI: 10.1175/JPO-D-11-0156.1

consequently its influence is often underestimated. A lateral circulation can be superimposed on the main flow axis, with upwelling over the deeper part of each section and downwelling near the sides (e.g., Winant 2008, for constant density with tides and rotation). These tidally induced residuals have the same order of magnitude as the density-driven flow and therefore are important in understanding estuarine dynamics. Furthermore, the residuals are not constant along the estuary, decreasing in magnitude with distance toward the head (e.g., Cheng et al. 2010). Wind can also enhance or repress the gravitational circulation by straining the along channel salinity gradient. Both residual flow and stratification have been highly correlated with wind forcing (Scully et al. 2005). This is another asymmetric straining process, causing stratification to always be reduced by an up-estuary wind. However, a down-estuary wind initially increases and then decreases stratification as the wind stress strengthens. The transition stage is a competition between wind straining and direct wind mixing (Chen and Sanford 2009).

The influence of tides on the residual circulation in stratified conditions is typically separated into three main effects (Cheng and Valle-Levinson 2009). First, tides create residual currents (even for unstratified cases, see for example Winant 2008) that modify the density-driven circulation. For tidal channels with relatively strong mixing the residual currents are seaward at all depths. Second, in tidal estuaries, tidal straining destabilizes the water column during flood tides and increases stratification during ebb tides, generating variable vertical mixing over the tidal cycle (Simpson et al. 1990). Finally, tidal dispersion affects the longitudinal salinity gradients, which are the drivers for gravitational circulation. However other parameters, such as distance to the head of the estuary (e.g., Li and O'Donnell 2005), may also affect residual circulation.

Estuaries essentially have a three-dimensional current structure, with the transverse current being as important as the longitudinal current; for wide estuaries Earth's rotation also needs consideration (Kasai et al. 2000). The channel-shoal bathymetric profile can also alter the conventional vertical two-layer exchange flow, with inflow in the deep channels and outflow over the shoals (Wong 1994). For a more comprehensive review of the physics of partially mixed estuaries the reader is referred to MacCready and Geyer (2010).

Analytical models are commonly used to describe patterns in physical estuarine processes by the use of numbers such as the Ekman number and Kelvin number. In these simplified models, important assumptions are made and temporal and spatial variations are neglected (e.g., Valle-Levinson 2008; Valle-Levinson et al. 2003). Classical threshold values for horizontal Richardson number, indicating the switch from periodic to permanent stratification may also only be valid for special cases (e.g., Burchard 2009). Although convenient, these assumptions can only describe essential features and can be very restrictive in dynamical macrotidal environments. Extensive areas of wetting and drying modify an estuary's cross channel profile, causing tidal variation in stratification and turbulence, and changes in residual circulation (e.g., Fortunato et al. 1999), which requires three-dimensional modeling. Therefore, a better strategy is to compare different physical influences, captured through modeling, with observations as suggested by Burchard and Hetland (2010).

The main objective of this research is to assess the impact of tides, winds, river-induced stratification, and Earth's rotation on the circulation in a macrotidal estuary. For this purpose, a three-dimensional model has been implemented in the Dee Estuary. Validation has been carried out by model–observation comparisons for salinity, which is the main control for density, surface elevation, current, and turbulence to fully assess the skill of the modeling system.

In the next section the Dee Estuary is presented. Section 2 describes nondimensional numbers that are commonly used to characterize estuarine dynamics. Section 3 describes the modeling system and its setup for this estuary. Section 4 shows the available data and characterizes the environmental conditions. Section 5 presents the application of the nondimensional numbers to the Dee Estuary, model results and discusses the relevance of tidal forcing, the river input and the pulses of residual circulation. Finally, section 6 presents the concluding remarks.

b. *The Dee Estuary*

The Dee is a macrotidal, funnel-shaped estuary situated in the eastern Irish Sea (Fig. 1) at the southeast corner of the Liverpool bay. It is about 30 km long, with a maximum width of 8.5 km at the mouth. The average tidal prism is 4×10^8 m^3, with a mean annual river discharge of 31 m^3 s^{-1} (peak flows can reach 300 m^3 s^{-1}), making the Dee Estuary tidally dominant. The ratio proposed by Schults and Simmons (1957) of the river inflow during a tidal cycle and the tidal prism is ~0.003, which would suggest a well-mixed estuary type; however, as shown in next sections, this is not the case and thus this ratio threshold does not apply for the Dee Estuary. The mean spring tidal range at Hilbre Island (located in Fig. 1) is approximately 10 m; this significantly extends the intertidal areas. Current velocities can be more than 1 m s^{-1} in the tidal channels occurring between high and low tide (standing wave). Many processes are time-dependent responding to tidal forcing, the eddy viscosity ranges from 0.001 to 0.03 m^2 s^{-1} and

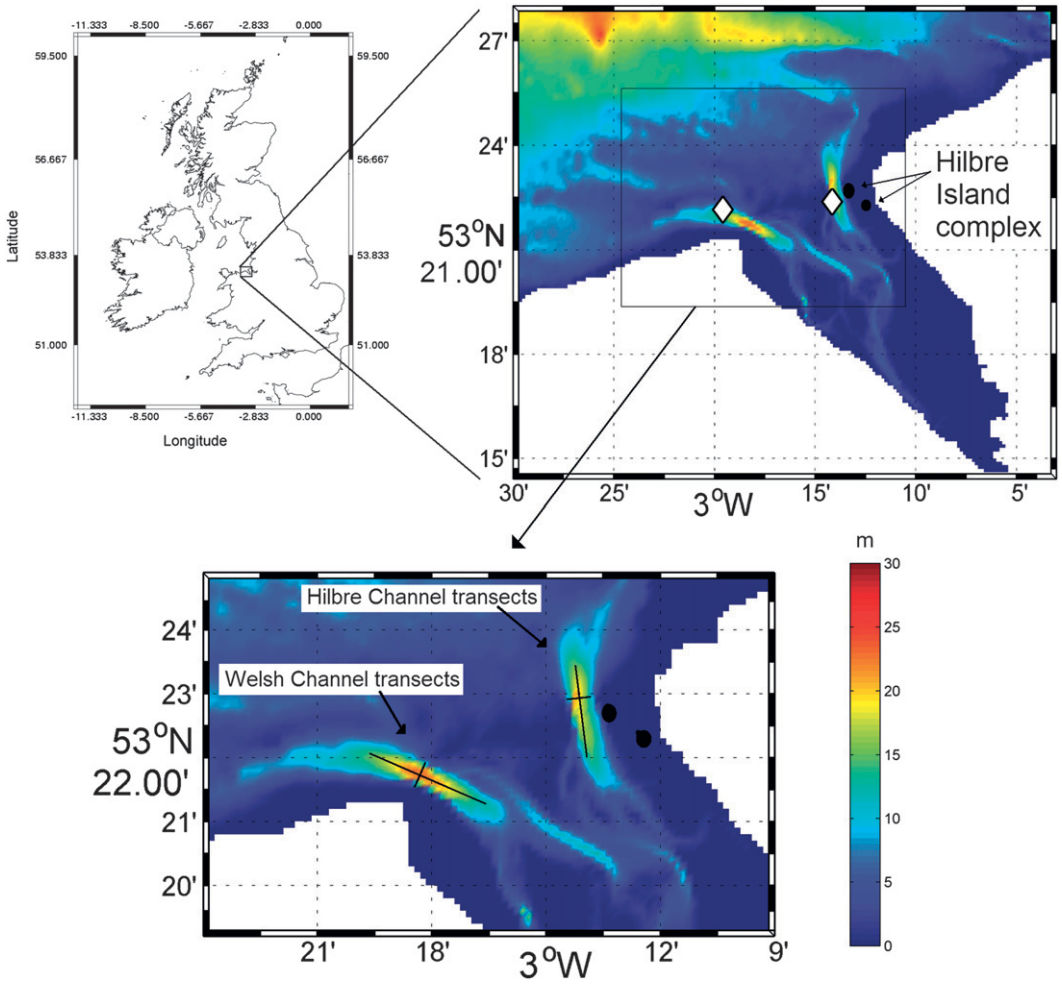

FIG. 1. The Dee Estuary located in southeast corner of Liverpool Bay, showing the (top right) bathymetry and the monitoring locations (white diamonds) in the Welsh (west) and Hilbre (east) Channels. (bottom) The location of the model transects output is shown.

the Ekman number ranges from 0.0138 to 1.15. The pattern of residual circulation is therefore expected to pulse with the tide.

The main estuary channel bifurcates 12 km seaward from the canalized river, resulting in two deep channels, ranging from about 20- to 30-m depth depending on the tidal phase, which extend into Liverpool Bay (Fig. 1). The Hilbre Channel is on the east and the Welsh Channel is on the west. Although the Dee imports sediment (Moore et al. 2009), it is suggested that it could be reaching a morphological equilibrium and that future accretion rates may decrease.

2. Estuarine classification by nondimensional numbers

Nondimensional numbers are commonly used to describe, in a generalized way, the properties of an estuary. They normally represent ratio values of different processes/factors and thus outline, in principle, the main dynamic characteristics. We have estimated five of the most common numbers to place the Dee in context of other estuaries and assess the applicability of such parameters for a macrotidal bifurcated estuary. The numbers used here and estimated in section 5a are as follows.

(i) The Ekman number shows the competition between friction and Earth's rotation. Coriolis effects become negligible at high Ekman numbers (>1). Valle-Levinson (2008) found that the exchange flow is horizontally sheared under high frictional conditions (Ek > 1) independently of the basin width. The Ekman number is defined as

$$E_k = A_z/(fH^2). \quad (1)$$

(ii) The Wedderburn number quantifies the relative importance of wind stress and baroclinic pressure gradient, and it is defined as

$$W = (\tau_w L)/(\Delta\rho g H^2). \quad (2)$$

(iii) The Kelvin number compares the basin's width with the Rossby radius. Earth's rotation effects are supposed to be more important when the Kelvin number >1:

$$K_e = B/R_{\text{in}}. \quad (3)$$

(iv) The Simpson number [equivalent to the horizontal Richardson number (Burchard and Hetland 2010)] measures the importance of stratification on mixing. The classical threshold value for separating periodic stratification from complete stratification is 2.1×10^{-3} (Simpson et al. 1990). The Simpson number is defined as

$$S_i = (\partial xb H^2)/(U_{\max})^2. \quad (4)$$

(v) The Strouhal number compares the water depth with the oscillatory bottom boundary layer. For large values of the Strouhal number the bottom boundary layer will not have time to reach the surface before it collapses because the tidal current reverses. It is defined as

$$\text{St} = H/(TU_{\max}), \quad (5)$$

where τ_w = wind stress along the channel, L = length of the channel, $\Delta\rho$ = density change over L, H = channel depth, ∂xb = horizontal buoyancy gradient, $U_{\max}$ = maximum tidal velocity, w = wind speed, T = tidal period, A_z = vertical eddy viscosity, f = Coriolis force, B = channel width, $R_{\text{in}} = (g'h)^{(1/2)}/f$, g = gravitational acceleration, g' = reduced gravity, and $b = -g(\rho - \rho_0)/\rho_0$ is the buoyancy, with $\rho_0 = 1000$ kg m^3.

3. The POLCOMS model

The Proudman Oceanographic Laboratory Coastal Ocean Modeling System (POLCOMS) is a three-dimensional numerical model formulated in a spherical polar, terrain-following coordinate system (sigma coordinates), on a B grid (Holt and James 2001). It solves the Boussinesq, hydrostatic equation of motion separated into depth varying and depth independent parts to allow time splitting between barotropic ($\overline{u}$) and baroclinic (u_r) components. The eastward velocity is $u = \overline{u} + u_r$, and the northward component is $v = \overline{v} + v_r$. For the inclusion of turbulence, POLCOMS is coupled to the general ocean turbulence model (GOTM; Umlauf et al. 2005), which includes several closure schemes. For the present work, the κ-ε scheme, using the stability function derived from Canuto et al. (2001), has been selected. For a detailed description of POLCOMS the reader is referred to Holt and James (2001) and Proctor and James (1996).

a. Model setup

To model the Dee Estuary, the POLCOMS-GOTM modeling system (Brown et al. 2010) has been extended to account for three-dimensional baroclinic effects. Freshwater river input, surface heating, and the offshore temperature and salinity structure have been considered.

Within Liverpool Bay, interactions of offshore (Irish Sea) water and river inflow cause periodic stratification. To capture the salinity and temperature conditions around the offshore model boundary a system of nested model grids was used (Brown et al. 2011). The Liverpool Bay domain (approximately 180 m resolution) was forced by boundary conditions (temperature, salinity, elevation, and currents) from Irish Sea simulations (approximately 1.8 km resolution) and by an initial condition for salinity of 35 PSU and for temperature of 7°C. Atmospheric forcing was generated by the Met Office Northwest European Continental Shelf (~12-km resolution, mesoscale) model, and comprised hourly wind velocity at 10 m and atmospheric pressure as well as air temperature, relative humidity, and cloud cover every three hours. Within POLCOMS, 15 tidal harmonics were considered for the tide only run. Daily averaged river discharges from the Environmental Agency river gauge network were made available from the Centre of Ecology and Hydrology (CEH) to include freshwater river sources within POLCOMS. In the absence of measured river salinity and temperature, default values of 0 PSU and seawater temperature were imposed at the river input location. The stratification and current field was spun-up over a month. For accurate modeling within the estuary, wetting and drying (Lane 2008) was considered. The best available bathymetry was used, which consists of digitized hydrographic charts combined with lidar data.

b. Numerical experiments

The model setup described above represents the reference simulation (P-ref). However, to quantify the effect of different processes several other simulations have been performed as detailed in Table 1. All simulations have the same open boundary conditions, but different forcings have been considered to investigate the local three-dimensional estuarine dynamics. The reference run (P-ref) includes full (atmospheric and river) forcing.

TABLE 1. Description of the model runs and physical processes included.

Run name	Tide	Atmospheric forcing	River	Coriolis	Stratification
P-ref	X	X	X	X	X
Ptide	X			X	
Pnostrat	X	X		X	
Pnoatm	X		X	X	X
PnoCor	X	X	X		X

Removing river input (Pnostrat) assesses the influence of the river-induced salinity stratification. A simulation considering river discharge but no stratification was performed, and showed that the river effect is due to the density gradient it creates and not its flow. This simulation is thus not discussed further. Atmospheric forcing is removed to gain insight into the wind-driven circulation (Pnoatm). A tidal alone simulation, without atmospheric forcing and river input (Ptide) is used to quantify the tidal influence, and finally, a simulation without rotation (PnoCor) is considered to assess the importance of Coriolis forces.

The numerical results are compared with observation and analyzed to estimate the relative contribution of the different processes. The statistical parameters used to quantify errors are

$$\text{percentage bias} = 100\frac{\sum_{n=1}^{N}(M_n - O_n)}{\sum_{n=1}^{N}|O_n|}, \tag{6}$$

$$D = 1 - \left[\sum_{n=1}^{N}(M_n - O_n)^2 \Big/ \sum_{n=1}^{N}(|M_n - \overline{O}| + |O_n - \overline{O}|)^2\right], \tag{7}$$

and the correlation coefficient (r^2), where M represents model data, O represents observation, and the over bar denotes the mean values. Percentage bias is the under or over prediction of the model compared with the observation considering values within 10% as excellent and 10%–20% very good. The index of agreement (D) is another quantity that measures the model skill and is bounded between 0 and 1, 1 being the optimum model.

4. Observations and environmental conditions

The observations used in this study are for a period with moderate waves, 14–29 February 2008 (Fig. 2), and provides a reasonable time to, first, perform model assessment and, second, to determine the physical processes occurring within the Dee Estuary. The data are

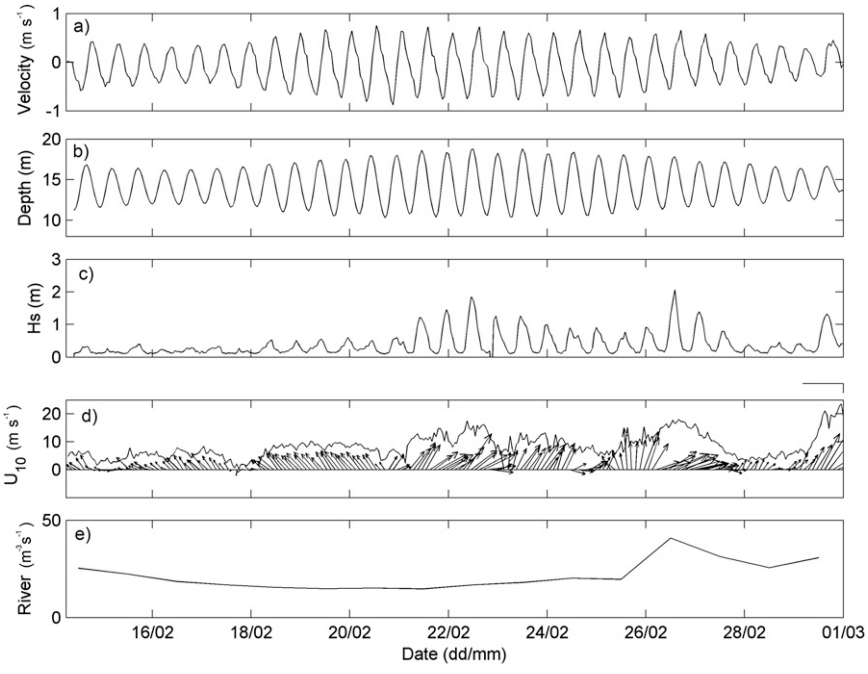

FIG. 2. Time series of observations at the Hilbre channel rig consisting of (a) near-bed current velocity (positive being ebbs and negative floods), (b) water depth, (c) significant wave height (Hs), (d) wind vectors and velocity at Hilbre Island, a few hundred meters from the Hilbre Channel deployment, and (e) river discharge.

from two locations close to the estuary mouth (Fig. 1). The first is in the Hilbre Channel, which consisted of a moored instrumented tripod deployed during mid-February to mid-March 2008 (Bolaños and Souza 2010). The mooring known as Sediment Transport and Boundary Layer Equipment (STABLE-III) is a tripod standing about 2.5 m high, with feet occupying a circle about 3.5 m in diameter, and weighing about 2500 kg (Williams et al. 2003). The mooring was equipped with several instruments to measure currents, waves, suspended sediment concentration, sediment size, salinity, and temperature. Data from an upward looking Acoustic Doppler Current Profiler (ADCP, from Teledyne RD Instruments) mounted on top of the rig are used here to obtain current velocity profiles and turbulence parameters with a vertical (bin) resolution of 0.5 m. Three Acoustic Doppler Velocimeters (ADVs) provided near-bed current velocities; however, ADCP data are used here as it provides a full water column description without frame interference (Bolaños et al. 2011). During the deployment, conductivity–temperature–depth (CTD) profiles were performed over 24 h every half hour starting from 1030 UTC 14 February 2008. The second location is the Welsh Channel where 24-h CTD stations were performed from 1400 UTC 12 February 2008.

In the Hilbre Channel (Fig. 2), the current velocity is dominated by tides, which follow the spring/neap and flood/ebb cycles, with slightly faster flood velocities in agreement with the tidal wave propagating in the shallow estuary. The flow aligns with the channel in a North–South orientation. Small waves are present and are modulated by the tide. At Hilbre Island, a few mild wind events with velocities of about 15 m s^{-1} are observed. Weak river flow (<25 m^3 s^{-1}) occurred during most of the study but increased toward the end (~ 40 m^3 s^{-1}).

5. Results and discussion

a. Nondimensional numbers

The use of nondimensional numbers (defined in section 2) requires the characterization of parameters describing the estuary. Channel bifurcation in the Dee makes the definition of width, depth, and estuary length somewhat arbitrary. We assess each channel independently and the results are presented in Table 2. The channel's dimensions are obtained from the transects shown in Fig. 1, for the channel width the 5-m contour was considered to represent the channel edge, while the channel length was defined by the 15-m contour. The Wedderburn numbers for both channels are relatively large in the down-estuary direction, with the Welsh channel being slightly larger as a consequence of the longer channel and slightly reduced horizontal density gradient. This indicates that the wind is expected to be more important for mixing in the Welsh Channel. However, this number does not give any information about the stratification itself. The Simpson number scales with the gravitational circulation; in the Dee this number is small for both channels indicating the presence of tidal straining. Similarly, the Strouhal number is small and of the same magnitude for both channels, showing the expected importance of the stratification. Burchard and Hetland (2010) presented residual velocity profiles for various combinations of S_i and St numbers showing the reduction of residual velocities with the reduction of both numbers. The Ekman number at both channels is 0.16 ± 0.03 indicating a transition from moderate frictional (<0.1) and high frictional (>1) conditions (e.g., Valle-Levinson 2008). In both channels the Kelvin number (<1) suggests Coriolis effect to have low importance on the baroclinic circulation. The lower value in the Welsh Channel is caused by the very weak stratification preventing the formation of a distinguishable buoyant surface layer from the influence of the near-bed salt wedge intrusion. In the next section stronger residual flows than that expected (<0.05 m s^{-1}), from the calculation of the nondimensional numbers, occur and even though both channels have similar dimensions they display different patterns of residual circulation.

TABLE 2. Channel dimensions (L, B, and H) and parameters used to estimate the nondimensional numbers described in Eqs. (1)–(5).

Parameter	Hilbre	Welsh
Length, L (m)	2660	3600
Width, B (m)	908	820
Depth, H (m)	22	24
τ_w (N m^{-2})	<0.15	<0.15
$\Delta\rho$ (kg m^{-3})	1.1	0.9
∂xb (s^{-2})	3×10^{-6}	2.4×10^{-6}
U_{max} (m s^{-1})	~ 1	~ 1
A_z (vertical eddy viscosity, m^2 s^{-1})	7.9×10^{-3}	1.3×10^{-2}
h (depth of buoyant part of flow, m)	5	10
Wedderburn	-1.68	-2.5
Simpson	1.5×10^{-3}	1.4×10^{-3}
Strouhal	5×10^{-4}	5.4×10^{-4}
Ekman	0.14	0.19
Kelvin	0.45	0.32

b. Surface elevation and currents

The modeled circulation is discussed in this section, focusing on the depth-averaged current, the vertical current structure, and the residual circulation within the estuary. The Hilbre channel ADCP is used for model validation before simulations are used to assess the residual

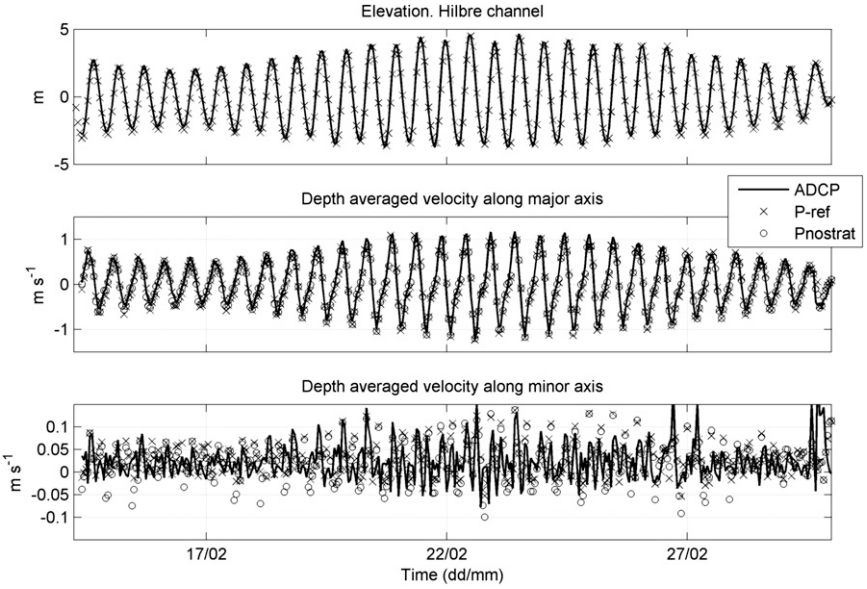

FIG. 3. Time series of (top) the observed (ADCP) and modeled surface elevation, (middle) the major component of the depth-averaged velocity, and (bottom) the minor component of the depth-averaged velocity at the Hilbre Channel mooring.

circulation along and across the tidal channels under different forcing processes. The model accurately predicts sea level elevations (Fig. 3, top panel) with a percentage bias of 12%, an index of agreement (D) of 0.98, and a correlation of 0.99. It has also been validated previously for surge in the Liverpool Bay area (Brown et al. 2011).

Modeled and observed depth-averaged velocities components have been rotated (Fig. 3, central and bottom panels) along their respective principal axis independently, to account for possible errors due to grid and bathymetry. The model reproduces the velocities very well, especially the major component. The minor axis component is overestimated and a reduction of the correlation coefficient occurs when the stratification is removed. The overall statistics (percentage bias, D, and r^2) for depth-averaged velocities obtained from different model runs are presented in Table 3. This table shows the simulations that have the most significant differences compared with the reference run. Considerably lower correlations and larger variance in errors among the model runs occur in the weaker minor depth-averaged component suggesting circulation induced by atmospheric forcing and rivers has stronger relative impact than in the major depth-averaged component, which is not very sensitive to the different processes modeled. The errors are comparable to the residual currents, discussed further in section 5e(1). As will be shown later, the Dee has large spatial variability, and thus errors in the model bathymetry may influence the present validation.

The depth-averaged flood and ebb currents for the reference run (Fig. 4) show intense, flood-dominant flow, which is more evident within the tidal channels. However, an ebb dominant flow is observed in the main channel near the head of the estuary. Within the estuary mouth, the weaker ebb flow is constrained to the Welsh Channel with less flow in the Hilbre Channel. Different behavior within the channels at the mouth occurs, bathymetric steering in the outer part of the Welsh Channel generates highly variable flow direction (Bolaños and Souza 2010). This, together with faster flows, may increase turbulence, bottom stress and mixing, reducing stratification in this channel (observed later in Fig. 6). A large spatial gradient is observed, especially at the channel edges, where velocities change dramatically within hundreds of meters.

A comparison of the observed (ADCP) and modeled (P-ref) velocities is presented for neap and spring tide (Fig. 5). During neap tide, the maximum velocities

TABLE 3. Statistic parameters: percentage bias (P bias), index of agreement (D), and correlation coefficient (r^2) for the depth-averaged minor (u) and major (v) velocity components in the Hilbre Channel for the investigated model runs.

	P-ref	Pnostrat	Pnoatm
P bias u (%)	15.9	−5.1	12.69
P bias v (%)	−9.5	−6.7	−7.7
D u	0.94	0.93	0.94
D v	0.97	0.98	0.97
r^2 u	0.4	0.34	0.4
r^2 v	0.97	0.97	0.96

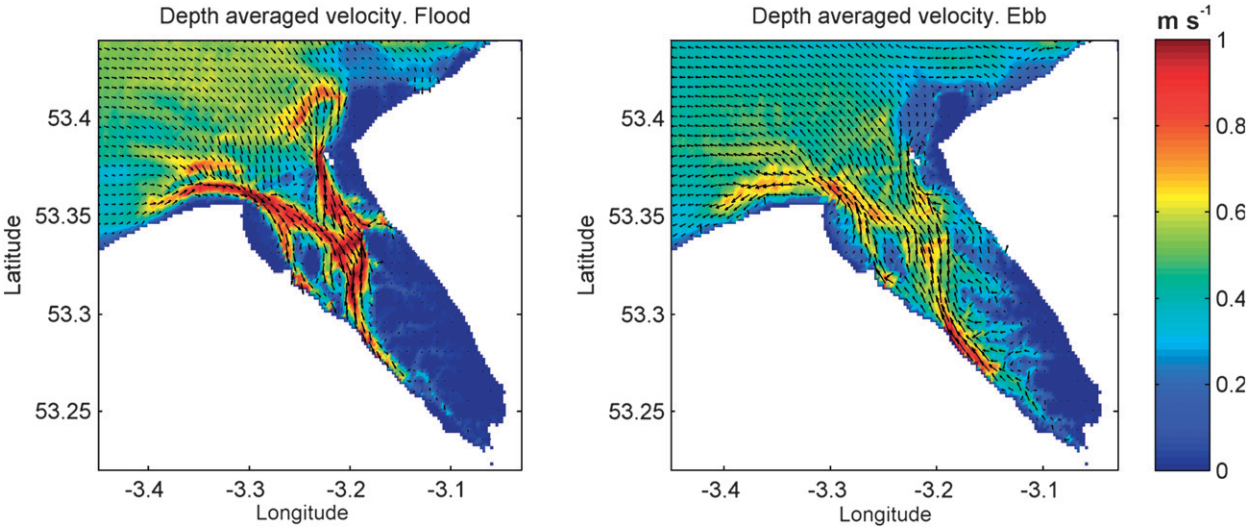

FIG. 4. Depth-averaged velocity distribution during (left) flood and (right) ebb during a neap tidal cycle. Similar patterns occur during spring tide but with faster magnitude.

($\sim$0.7 m s^{-1}) are accurately modeled, but stronger vertical shear occurs compared with the measurements. The observed tidal asymmetry, showing larger flood velocities, is not clearly reproduced by the model. During spring tide the observed velocities exceed 1 m s^{-1} and the flood and ebb phases become less asymmetric. The model underestimates the velocities, most noticeably during flood tide, and also simulates larger vertical velocity shear than that observed, owing to the underprediction of the bottom currents. The model produces ebb dominance during spring tides. The wind- and density-driven currents are an order of magnitude weaker (not shown) than the tidal currents, the effect of these processes is therefore not clearly observed in the velocity profiles, however, they have a significant impact in the residual circulation patterns as discussed in section 5e(1).

c. *Salinity*

The Dee is a tidally dominated estuary with small river inflow. However, stratification may develop influencing turbulence and transport processes. Figures 6a and 6c show the salinity profiles from the CTD stations in the Hilbre and Welsh Channels, respectively. Close to low tide in the Hilbre Channel, a lower salinity surface layer is present; near high tide the profiles become uniform with increased salinity. The flood currents increase salinity as the salt wedge moves into the estuary, while ebb currents decrease salinity and produce strong stratification, located close to the surface due to the tidal straining and river effect. The CTD casts in the Welsh Channel were farther offshore, causing offshore water to have more influence, giving rise to higher overall salinity values and reduced near-surface stratification at low water, suggesting that more mixing could be occurring. The salt wedge advances into the estuary shortly after the onset of the flood tide.

The stratification patterns between the channels differ somewhat (Fig. 6a and c). In the Hilbre Channel strong stratification occurs near the surface at low tide because of the effect of the river and tidal straining. However, a weak salt wedge is observed propagating into the estuary after low tide. In the Welsh Channel, intrusion of the salt wedge into the estuary causes the strongest stratification (weaker than the Hilbre Channel) to occur on the flood tide near the bed initially, before progressively moving toward the surface through time. Tidal straining of the horizontal salinity gradient is expected to be small in response to the weak river influence in this channel.

The modeled salinity profile in the Hilbre Channel (Fig. 6b) agrees relatively well with observation (Fig. 6a) during high tide, the model does predict a well mixed water profile, but the near-surface stratified low water profile is weaker than observed. The near-bed intrusion of the salt wedge is partially reproduced by the model. Stratification, estimated as the difference between the bottom and surface layers, is slightly underestimated: the model predicts a maximum difference of about 3 PSU while the observations produce a maximum difference of 4.5 PSU. In the Welsh Channel, the model (Fig. 6d) simulates a weaker vertical salinity gradient and different patterns to those observed. Stratification is also underestimated in the Welsh Channel, observed differences between bottom and surface show maximum values around 2 PSU while in the model it is around 1 PSU. This overly mixed vertical distribution could be attributed to the turbulence closure, which is explored further in section 5d, where the model is shown to overestimate the turbulent kinetic energy production (P).

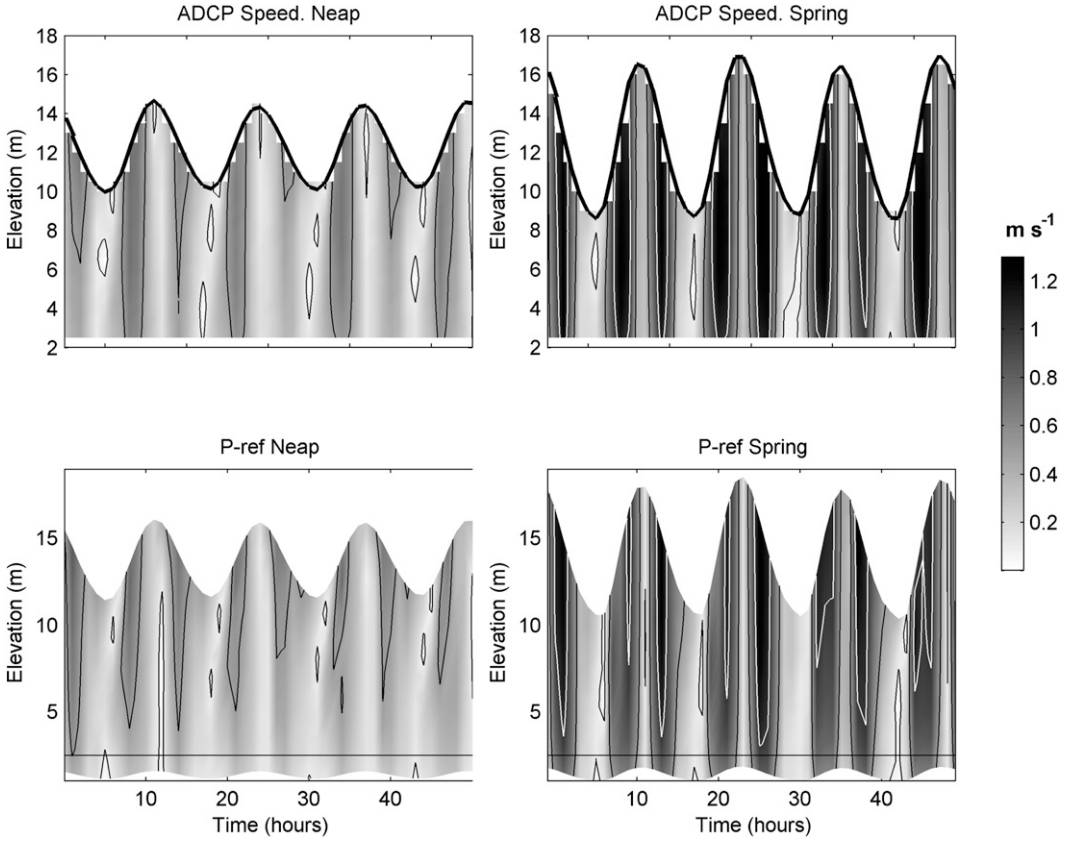

FIG. 5. (top) Measured and (bottom) modeled speed at (left) neap and (right) spring tides in the Hilbre Channel. The horizontal black line in the bottom plots shows the elevation at which the ADCP measurements begin. Velocity contours are at 0.1, 0.5 and 1 m s^{-1}, the 1 m s^{-1} contour is plotted in white for visibility.

d. Turbulence

Turbulence interacts with currents and affects the distribution of water masses within the water column. The current shear squared, defined as $(\partial u/\partial z)^2 + (\partial v/\partial z)^2$, and the turbulent kinetic energy production (P), defined as

$$-\rho\left[\langle u'w'\rangle\left(\frac{\partial u}{\partial z}\right) + \langle v'w'\rangle\left(\frac{\partial v}{\partial z}\right)\right],$$

where ρ is water density, u, v, w, are the velocity components and z is the vertical coordinate, derived from the Hilbre Channel ADCP are investigated (Fig. 7, first and second row). At low water neap tide a strong current shear is observed, associated with strong stratification (see Fig. 6a). The maximum P (Fig. 7b) occurs near the surface for low and high water but near the bottom during floods. At spring tide, large near-bed shear (Fig. 7c) occurs for the majority of the tidal cycle, extending to the surface at low tide and dropping in magnitude at high tide. The P (Fig. 7d) becomes flood dominant, with large near-bed values during floods and large values near the surface at high tide associated with the wind effects [explored in section 5e(1)]. Stratification asymmetry creates this imbalance, which enhances the density-driven circulation, as suggested by Jay and Smith (1990). Compared with density driven flow, the relative importance of flow induced by asymmetric tidal mixing decreases as stratification increases.

The model results are presented in Fig. 7 (third and fourth rows). The modeled pattern of low water neap current shear (Fig. 7e) agrees with the observations, however, the magnitudes are overestimated and the shear penetrates deeper into the water column. The simulated P (Fig. 7f) shows large near-surface values at low water, but maximum values are found near-bed during flood and ebb tide, the observed asymmetry is not reproduced. The P magnitudes are slightly over predicted. During spring tides strong near-bed and low tide surface shear and P (Figs. 7g,h) are modeled, with weak low tide near-bed and high tide surface P. Tidal asymmetry in the near-bed signal is lost and the P extends much further up into the water column.

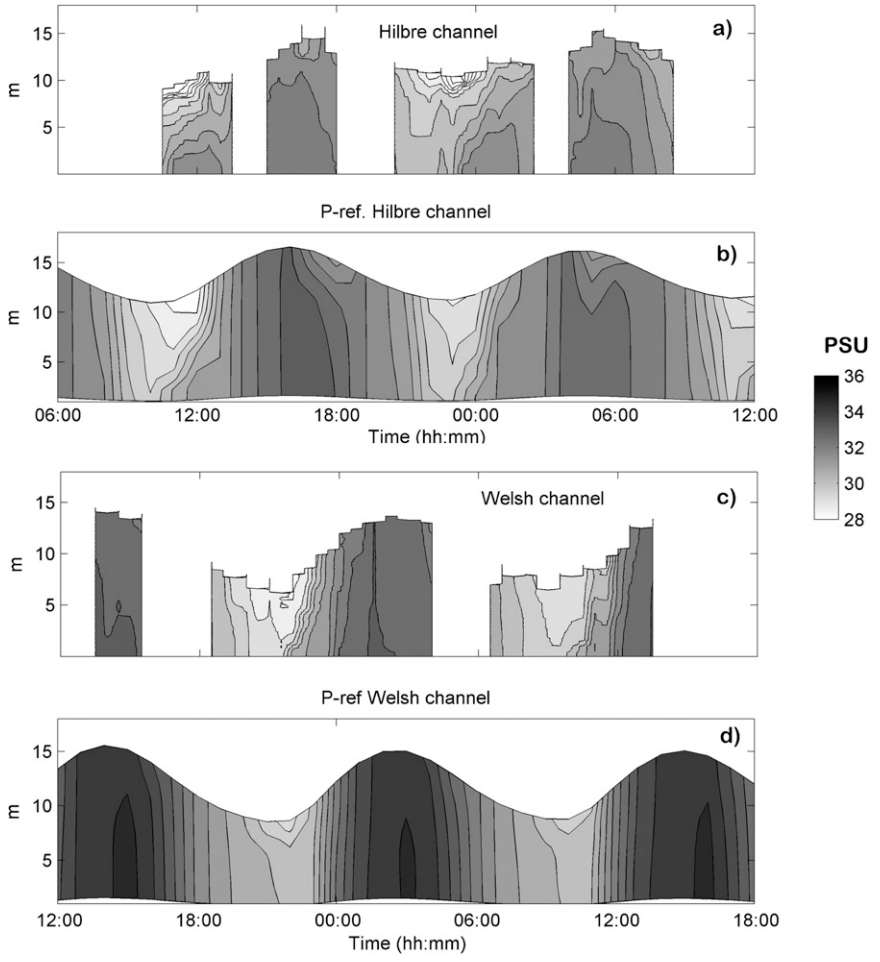

FIG. 6. Time series of salinity profiles from CTD casts during a neap period in (a) the Hilbre Channel and (c) the Welsh Channel. Strong currents, preventing CTD deployment, caused the gaps seen in the data. The casts were not simultaneous, hence the offset in observations between Hilbre (14 Feb 2008) and Welsh (12 Feb 2008) Channels. (b),(d) The salinity distributions for the reference (P-ref) simulation during the same times are shown. Contours are plotted in a 0.5-PSU interval.

The Dee can switch from being horizontally to vertically sheared depending on the tides. The eddy viscosity also changes within the tidal cycle showing tidal asymmetry and ranges from 0.001 to 0.03 $m^2 s^{-1}$. The tidal channel dimensions also change drastically with tidal phase (ebb or flood), therefore, the use of tidally averaged quantities to describe flows may be misleading owing to the asymmetric modulation of the baroclinic motions.

e. Numerical assessment of the effects of tides, river, wind, and Coriolis forcing

1) EFFECTS ON RESIDUAL CIRCULATION

The residual circulation is the portion of the currents not induced by the direct oscillation of the tidal flow and, for the residual profiles, has been defined as a time-averaged velocity using sigma levels. The observed and modeled residual circulation profiles in the Hilbre Channel are presented for the entire study period (378 h) and for two separate 100-h periods centered over neap and spring conditions (Fig. 8). The full period is therefore not equivalent to the combined spring and neap period considered here and is representative of a longer unclosed cycle. The observed major component shows the greatest vertical variability with a two-layer system, while both modeled components show considerable vertical variation with a strong two-layer system in the minor axis. Although the results for the minor-axis present larger errors, the model is useful to further understand the cross-channel circulation patterns. A clear improvement in the minor residual component occurs when stratification and atmospheric forcing are considered.

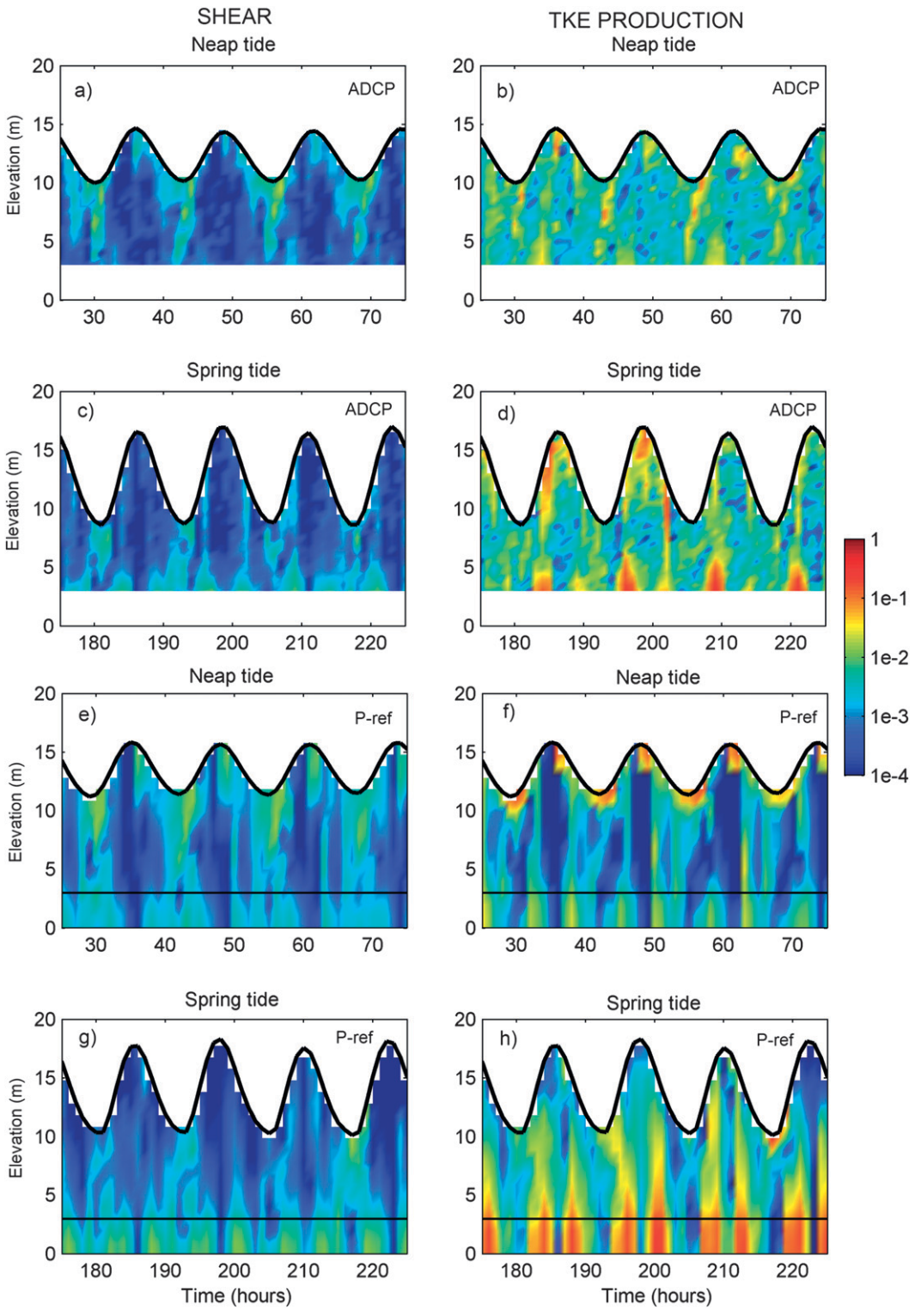

FIG. 7. (left) Current shear ($m^2\ s^{-2}$) and (right) TKE production (P, W m^{-3}) from (a),(b),(c),(d) ADCP and (e),(f),(g),(h) model in the Hilbre Channel during (a),(b),(e),(f) neap and (c),(d),(g),(h) spring tides.

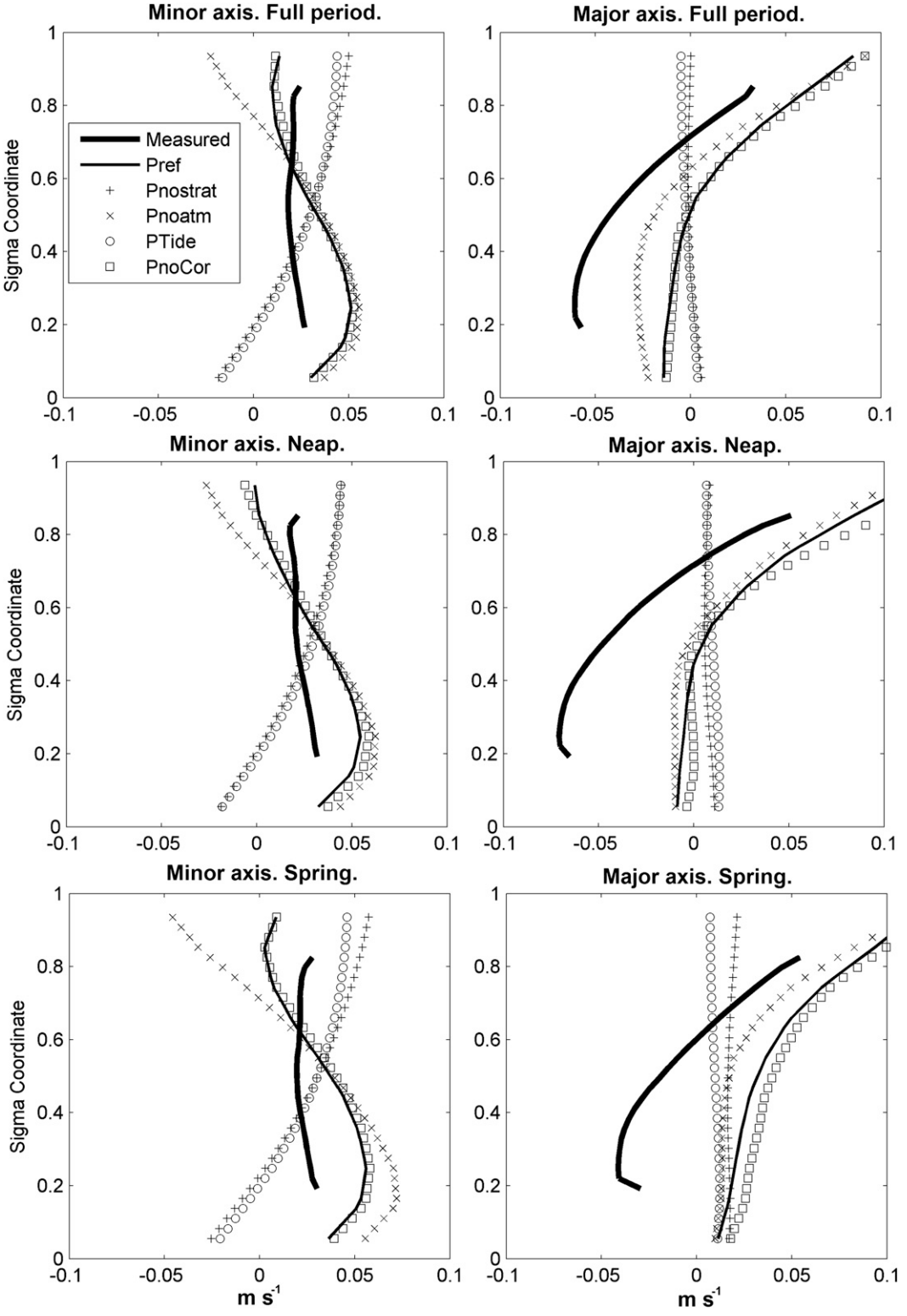

FIG. 8. Residual circulation profile from observed ADCP data (mounted on the Hilbre rig) and modeled data under different forcing terms, given in Table 1. (top) The full studied period, (middle) neap period, and (bottom) spring period are shown. Positive values indicate flowing out along channel for major current component and flowing toward the right bank (for a viewer facing toward the offshore flow direction) for the minor axis component.

All the runs with stratification have the same vertical pattern in the major component, with an overestimation of near-surface velocity and underestimation of near-bed velocity. The residual varies within the spring-neap cycle creating an unsteady pulsing flow. The pulses are later shown to additionally occur within a tidal cycle.

Here, the effect of the tides in the absence of atmospheric forcing and river flow is first analyzed. Tides by themselves (Ptide) are not able to produce a strong residual in the major axis circulation at the Hilbre location. Both components show near-bed flow reversal for the full period. However, it is noted that during isolated spring and neap tides the major axis profiles does not show such reversal. This results due to the full period consisting of more than a single closed spring and neap cycle. The time-average is therefore biased because of partial consideration of a tidal phase mainly observed in the runs that are strongly controlled by tide only processes.

Atmospheric forcing in addition to tides (Pnostrat) compared with the tide alone (Ptide) simulation highlights the importance of surface wind forcing in producing residual circulation. For both neap and spring tides the wind influences the entire water column, although most of the impact is concentrated at the surface and a stronger effect is observed during spring tides due to the occurrence of a wind event. The effect of the wind at the surface is enhanced in the presence of stratification (cf. the difference between Ptide and Pnostrat with the difference between Pref and Pnoatm), due to the boundary between the two layers.

By considering tides and river-induced stratification (Pnoatm), the importance of stratification (when compared to Ptide) in increasing vertical current shear and creating a two-layer flow system is observed. The greatest impact occurs for the across-channel residual, for which spring tide generates a more pronounced two-way flow. However, the modeled major residual components during spring tides exhibit unidirectional flow throughout the water column, and do not reproduce the two-layer system. This is contrary to neap tides when the effect of the river is observed to produce an offshore flow in the top third of the water column and an onshore flow in the bottom. In general all the runs present a systematic bias of the current residual profile indicating an overestimation of currents going out of the estuary (or underestimation of the current coming into the estuary) by an order of 0.03 m s^{-1}. This can be attributed to errors in tidal propagation within the domain producing the less evident errors in the depth-averaged velocity shown in Fig. 3.

Earth's rotation has generally the weakest impact on the residual in both components. Without rotation (PnoCor), the residual profile slightly deviates from the reference run (P-ref), especially at spring tides for faster flow conditions, thus generating an across-channel asymmetry. The major axis component without Coriolis gets enhanced owing to the fact that the outflow is no longer pushed toward the right side of the channel and thus, an intensification occurs in the west side (where the observations were performed). This is in qualitative agreement with the work of Winant (2008) and Lerczak and Geyer (2004) that showed the rotation altered the tidally induced flows. However, specific changes depend on the model setting and the position with respect to the longitudinal and axial channel axes. The sign of the model variations due to Coriolis forcing agree with those of Winant (2008) for an intermediate effect of friction on a transect at the center of the channel.

Overall, processes related to density gradients are essential for accurately modeling residual circulation. By considering all of the above processes the general patterns of the residual circulation have been modeled, but the major component is overestimated near the surface and underestimated near the bed, and vice versa for the minor residual component. Such errors could be related to simulation of the stratification and turbulence fields and also to spatial gradients in bathymetry. The spatial variability of the modeled residual circulation is large, hence any slight discrepancy in the rig positioning in relation to the bathymetry may produce large variations in the residual pattern. For this reason the use of flexible meshes has to be considered in future studies in order to increase spatial resolution in the tidal channel edges.

To gain insight into the residual circulation patterns within the Dee, the spatial distribution of the bottom and surface residual, obtained from the vertical model level above the bed and below the surface, for simulations with and without stratification are compared (Fig. 9, top and central panels). Large spatial variability in magnitude and direction occur. An intense offshore surface flow in the outer Welsh Channel is persistent in both runs, with slight intensification when considering stratification. In the outer Hilbre Channel, without stratification the residual flow at the surface is onshore, however, with stratification this pattern changes to offshore. Maximum residual velocities occur at the surface in the tidal channels reaching 0.2 m s^{-1}. Similar patterns are found near the bottom, but with lower magnitudes, reaching 0.1 m s^{-1} and weaker spatial gradients. The clear near-bed bidirectionality in the Hilbre Channel occurs only in the outer part of the channel and is a result of tidal, barotropic, and bathymetric interactions, while the near-bed offshore flow in the Welsh Channel is due to lateral shear in the tides alone. In the upper estuary differences between runs are small, with larger effects

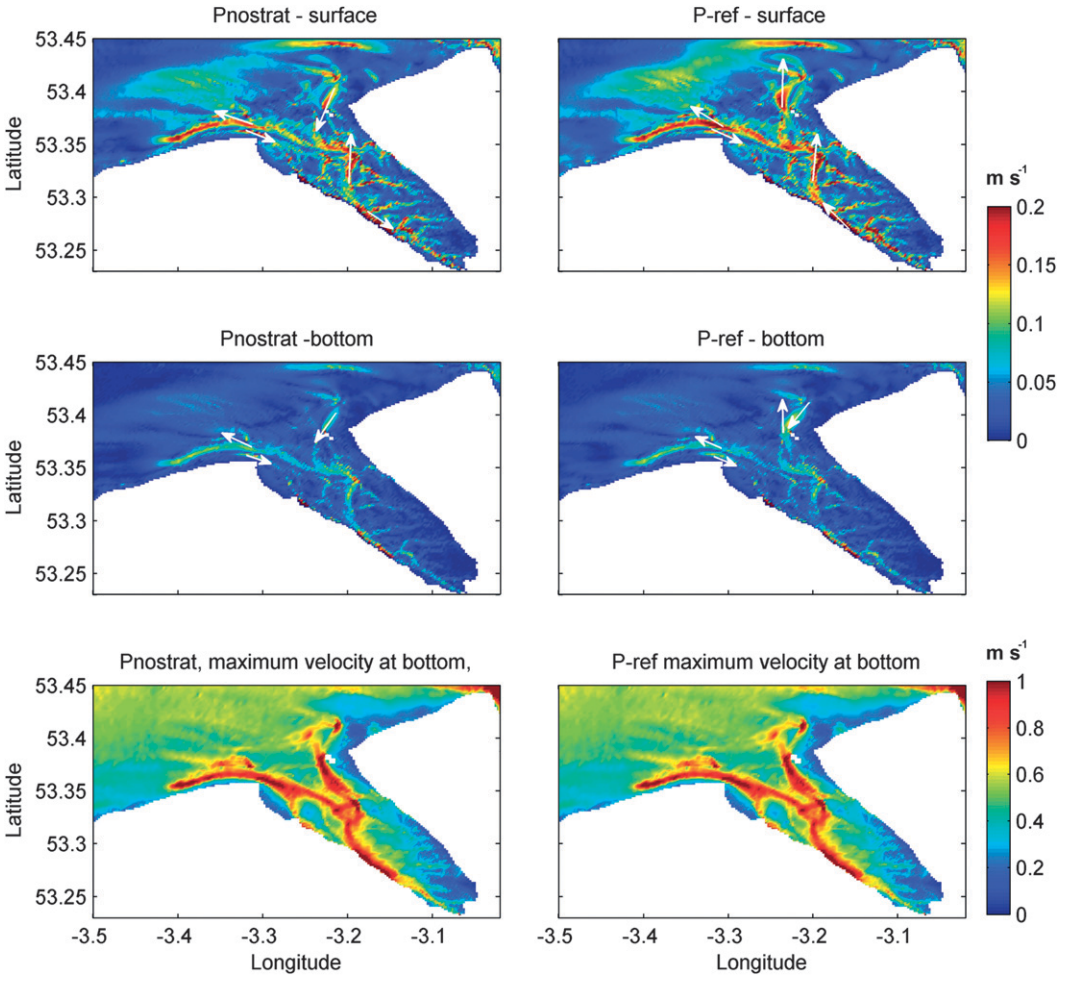

FIG. 9. Distribution of (top) surface, (middle) near-bed residual circulation, and (bottom) the maximum near-bed velocity for simulations (right) with (P-ref) and (left) without (Pnostrat) stratification.

observed closer to the estuary mouth. Maximum near-bed velocities at each model grid point are also shown (Fig. 9, bottom panels). Although the residual currents influence the transport pathways of suspended particulates, the maximum bed velocities have a direct effect on resuspension of material from the bed. The transport of material is therefore dependent on the stratified conditions influencing the residual. The maximum velocities occur in the tidal channels, reaching 1 m s^{-1}, and are unaffected by stratification.

The large spatial changes (e.g., Fig. 4 and 9) reflect the spatially varying physical processes and bathymetry; large velocity gradients at the edges of the channels are particularly noticeable. A small error in model bathymetry (e.g., erroneous position of a channel) could modify the validation shown in Fig. 3, 5, and 8. Thus, bathymetry plays a crucial role in obtaining accurate predictions as also shown by Wang et al. (2009) and Plant et al. (2009).

The modeled major and minor residual circulation components, at transects shown in Fig. 1, are compared to determine the influence of stratification and evaluate the processes taking place in the area. The Welsh and Hilbre Channel experience very different flow patterns for the reference run (Fig. 10). The Welsh cross channel section has a horizontal structure in the residual current (Figs. 10a,b), which flows out (NE) along the right bank and in (SW) along the left bank. This pattern agrees with the case of low friction and wide basins described by Valle-Levinson (2008), in which results have been obtained by modeling stationary conditions. However, the discrepancy with their K_e and E_k numbers suggest other sources of residual circulation, which could be due to bathymetric features or wave processes. The along channel transect (Figs. 10c,d) also shows some horizontal structure, more evident in the major residual component. This structure is due to the curvature of the Welsh Channel, which bends toward the west, while the

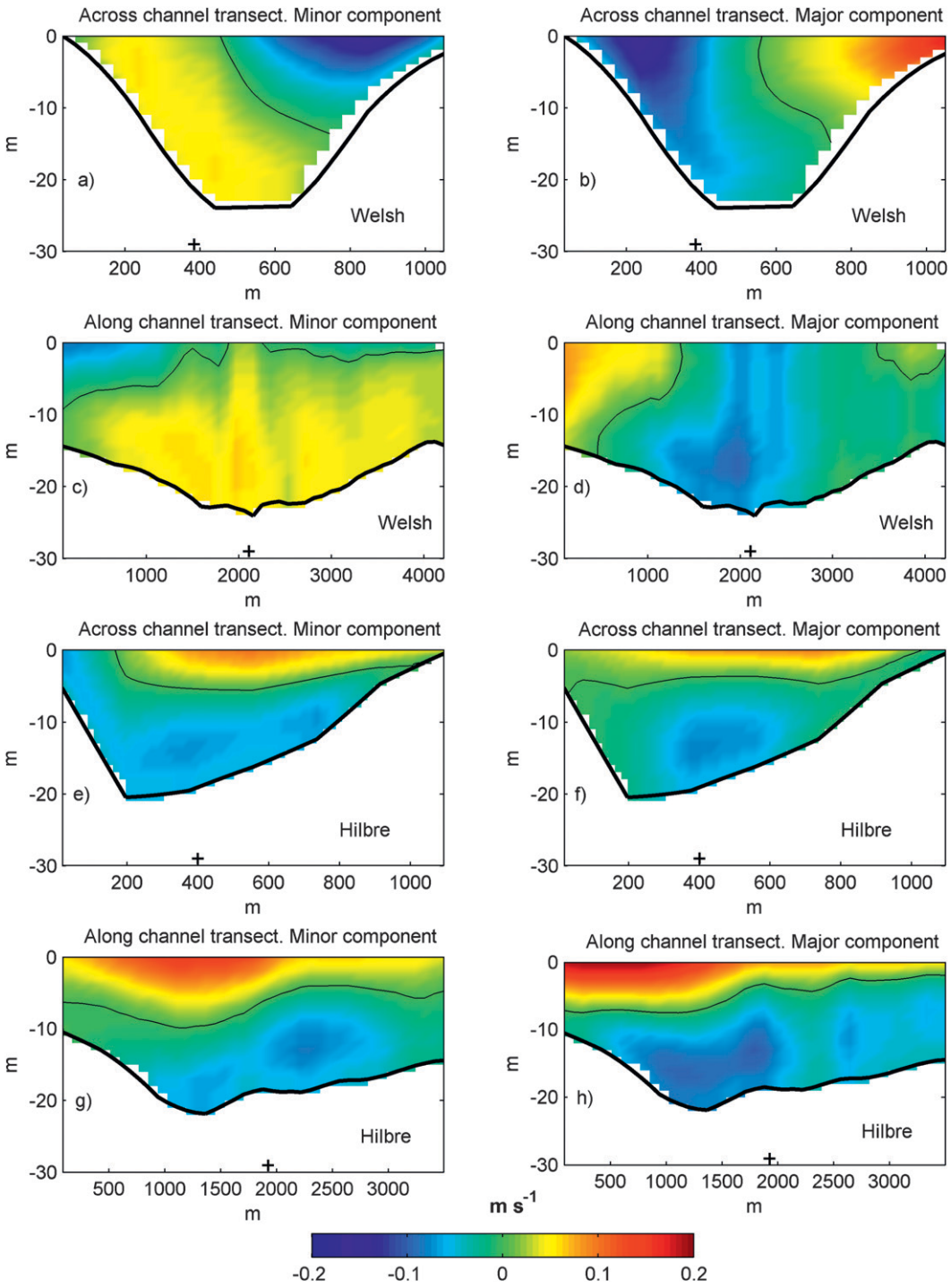

FIG. 10. Transects of residual circulation for the reference run (P-ref) for (a),(b),(c),(d) Welsh Channel and (e),(f), (g),(h) Hilbre Channel. Positive values for minor component are currents flowing across a channel from left to right (looking from estuary to offshore). Positive values in the major component are currents flowing along the channel out of the estuary. Across channel transect go from SW to NW and the along channel transect from NW to SW. The "+" indicate the horizontal position where transects cross.

along-channel cross-section is straight, thus cutting across the boundary between the opposing flow directions and forming the cross-channel residual circulation. The Hilbre Channel (Figs. 10e,f,g,h) presents a clear two-layer system in which the surface layer flows out (NE) of the estuary and bottom layer into (SW) the estuary. In the across-channel transect, the minor component (Fig. 10e) is slightly shifted to the right side of the channel because of the combined effect of Coriolis and bathymetric features.

In the absence of stratification (Fig. 11), virtually the same pattern as tide alone conditions occurs (not shown). Density gradients are therefore the dominant forcing in the residual circulation compared with river flow and atmospheric influence during this calm period. The absence of stratification changes the modeled circulation, particularly in the Hilbre Channel. In the Welsh Channel the lack of river-induced stratification produces a horizontally sheared residual flow (similar to the P-ref run) with the boundary between the inflow and outflow located in the center of the channel, suggesting that this location is dominated by tidal processes. Without stratification the Hilbre Channel has a similar structure to the Welsh Channel, a horizontal structure completely different to the vertical two-layer system, suggesting the residual circulation of this channel is dominated by density-driven processes. Although the river input is small, the resulting horizontal density gradient and the marked stratification during low tide, considerably alters the flow. The changes are in response to (i) the horizontal pressure gradients and (ii) the asymmetries in turbulence production by enhanced intertidal stratification (related to tidal straining). The modeled turbulence asymmetry is weaker than that observed; the density-driven circulation may therefore be underestimated, which could explain the errors found in the residual circulation profiles (Fig. 8).

The effect of the wind on the residual transect circulation (not shown) is relatively small. In both channels the depth of the surface layer is increased through enhanced surface mixing. For more than half the study period, and when wind events were largest, the wind direction was from SW (between 180° and 270°). This direction forces river water toward the east and enhances the surface outflow, enhancing the estuarine and Coriolis induced circulation in the Hilbre Channel. In the Welsh Channel the vertical boundary between the inflow and outflow is only slightly shifted toward the east of the channel.

Inter-tidal variations in channel profile and turbulence can induce pulses in the residual circulation. Thus, the timing of stratification in relation to the tidal cycle is important (Stacey et al. 2008). In the Dee the tidal elevations change the wet estuary width from about 7 to 2 km, split into two 1-km channels separated by dry banks. The river flow is fairly constant during the study but is constrained by intertidal banks within the tidal cycle. These bathymetric changes within the intertidal period are expected to change the relative importance of the river. By studying the Hilbre Channel, a macrotidal channel with significant river-induced stratification, the tidally influenced changes in the residual due to stratification are found to be stronger at low water (larger, positive, surface outflow), when the river is constrained within the channel and tidal currents are weak enabling the greatest stratification (Fig. 12, top panels). The influence is greatest during neap tide in the surface and bottom layers, with little change mid depth, while at springs the outflow pulses occur over deeper layers in the water column (full water column at low tide). This outlines the importance of the tidal variation produced by turbulence and stratification. During low tide the effect of the river is stronger and more persistent, and thus, pulses in circulation occur around these periods. It is also possible to observe a common feature in the whole water column characterized by an up-estuary pulse at the beginning of the ebb, when weak stratification and horizontal gradients occur, and also a surface pulse during the peak of the flood, these features might be explained by a horizontal density gradient within the tidal propagation.

Wind can also produce pulses in circulation owing to changes in its direction, intensity, and the interaction with stratification (Figs. 12 and 13, central panels). Observed winds at Hilbre Island were less than 10 m s^{-1} during the neap period and about 15 m s^{-1} during the spring period. The wind-induced pulses were therefore greater during spring tide in response to an increase in wind speeds, and not the phase of the spring-neap cycle. However, the effect of the wind forcing is tidally modulated, with larger effects near high slack water, close to the surface. At high water the wet areas over the estuary are greater owing to bank inundation allowing the wind to have greater influence because of the larger area on which it acts.

Earth's rotation may be particularly important in wide estuaries. It can produce asymmetries between in and out flow and also destabilize the water column (e.g., Winant 2008; Lerczak and Geyer 2004). In an estuary with large tidal amplitude, the width of the estuary may be highly variable; this can produce pulses due to the different relative importance of Earth's rotation within a tidal cycle. Figures 12 and 13 (bottom panels) show the effect of Coriolis (the difference between P-ref and PnoCoriolis) has significant changes within the tidal cycle. The figures show some correlation of the effect

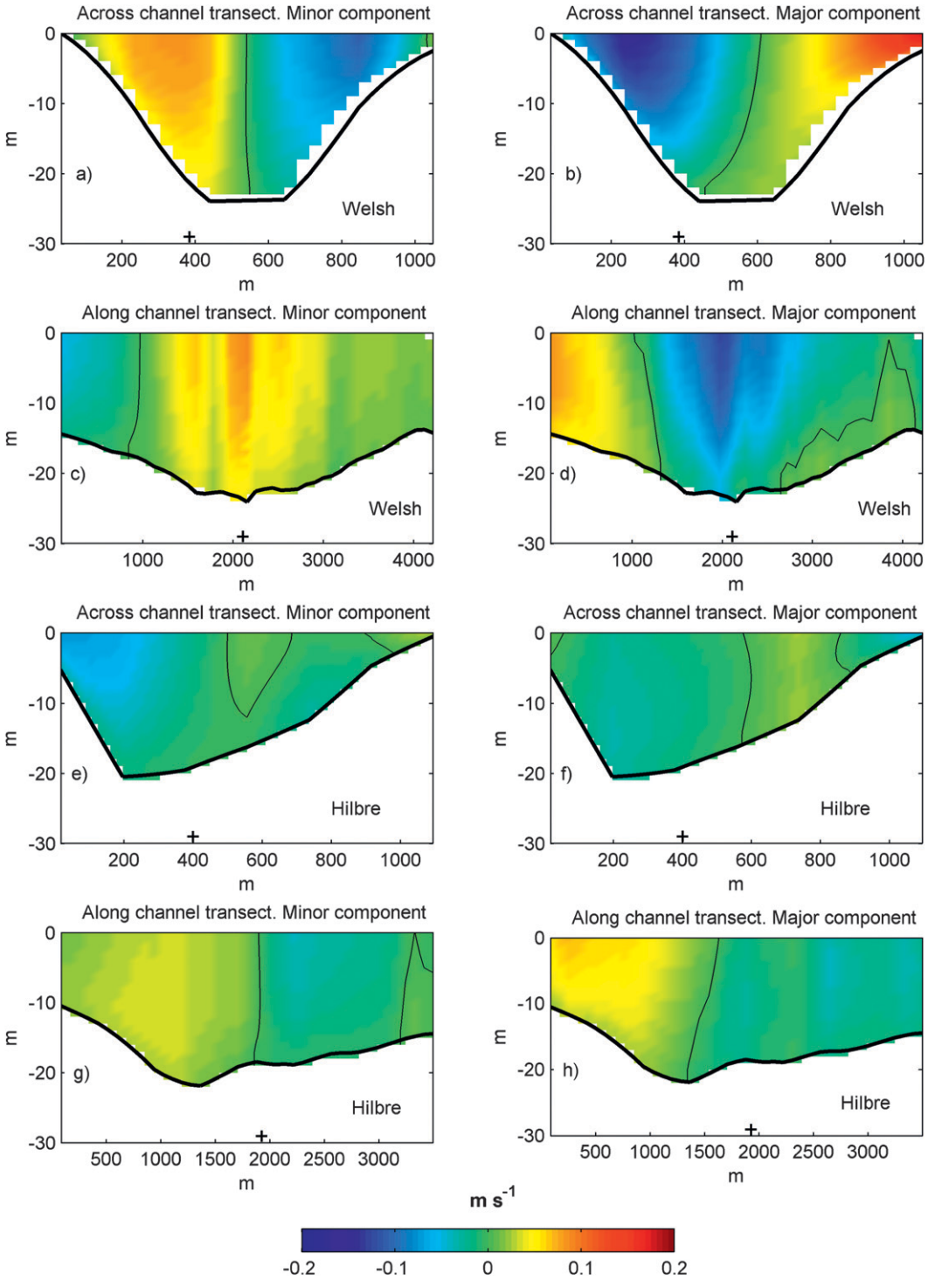

FIG. 11. As in Fig. 10, but without river input (Pnostrat).

with the tidal phase and differences between neap and spring are observed. The effect on the minor component during neaps is related to the flood and ebb as Coriolis produces altering current direction for different tidal phases. For the major component the effect is related to low and high water, associated to the constraint of the river water. During the spring tide the effect on the minor component seems to be reduced at ebbs; this is due to the presence of the SW wind event that enhances estuarine circulation, thus counteracting the Coriolis

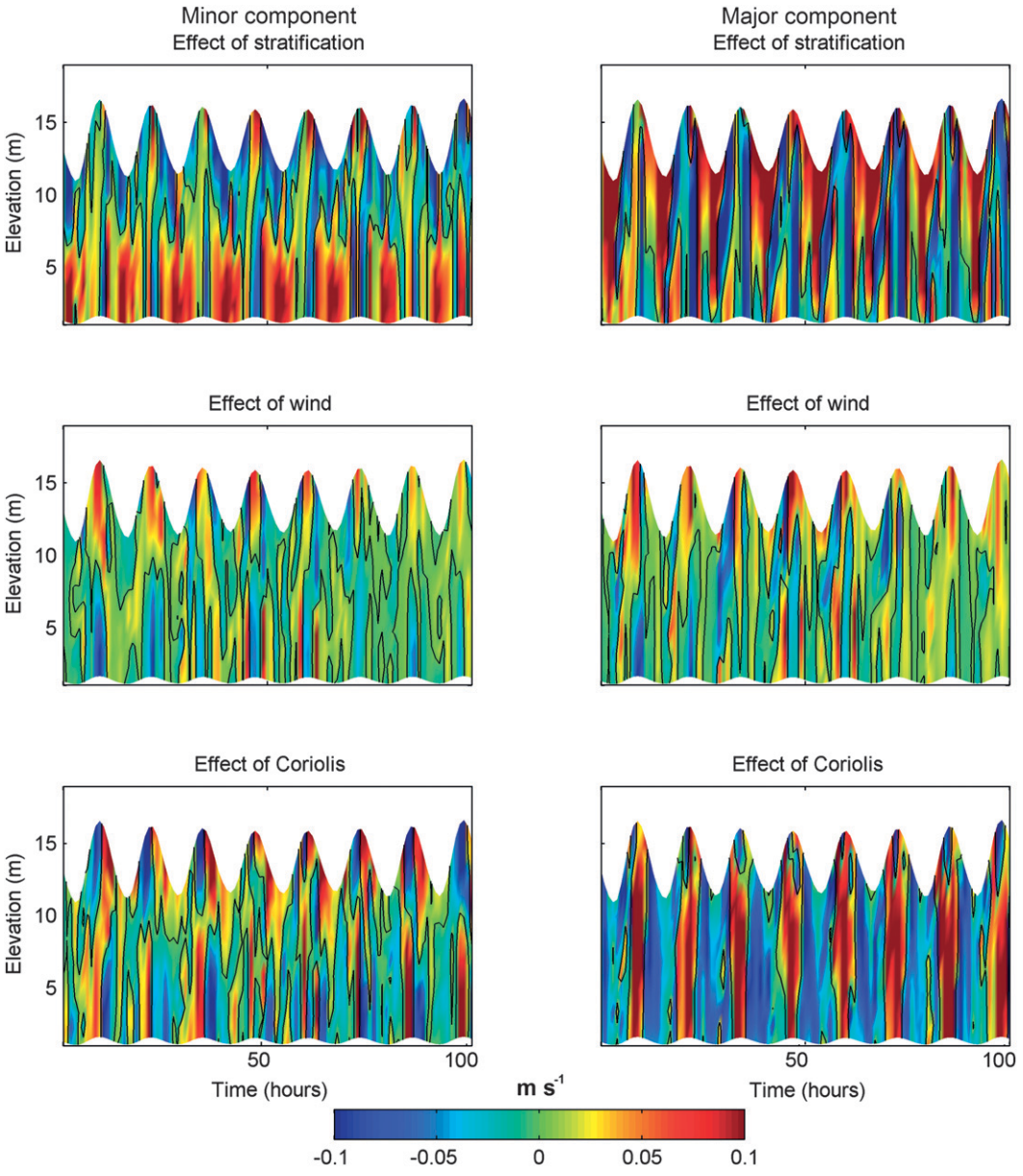

FIG. 12. The effect (estimated by the difference between the reference run and the run without the particular forcing) of (top) stratification, (middle) wind, and (bottom) Coriolis on the (left) minor and (right) major current component for a neap period at the Hilbre Channel station. Units in m s^{-1}.

effect. The influence of Coriolis is not only a direct modification of the current; it can also change the density distribution and thus the gravitational circulation.

2) ALONG- AND ACROSS-CHANNEL SALINITY DISTRIBUTION

Salinity distributions along and across the channels are investigated (Fig. 14) at low tide, when stratification is greatest and differences between spring and neap tide are most apparent. A clear along channel gradient is observed (Figs. 14c,d,g,h) with increasing salinity toward the mouth, with fresher water at the surface closer to the river source. The across channel profile (Figs. 14a,b,e,f) shows the surface freshwater is forced toward right of the channels, with salty bottom water extending toward the surface along the left of the channels. Without Coriolis (not shown) this shift does not occur. During neap tides the salt wedge in the Hilbre Channel has greater influence, creating saltier profiles. During spring tides, lower water levels at low tide allow river water

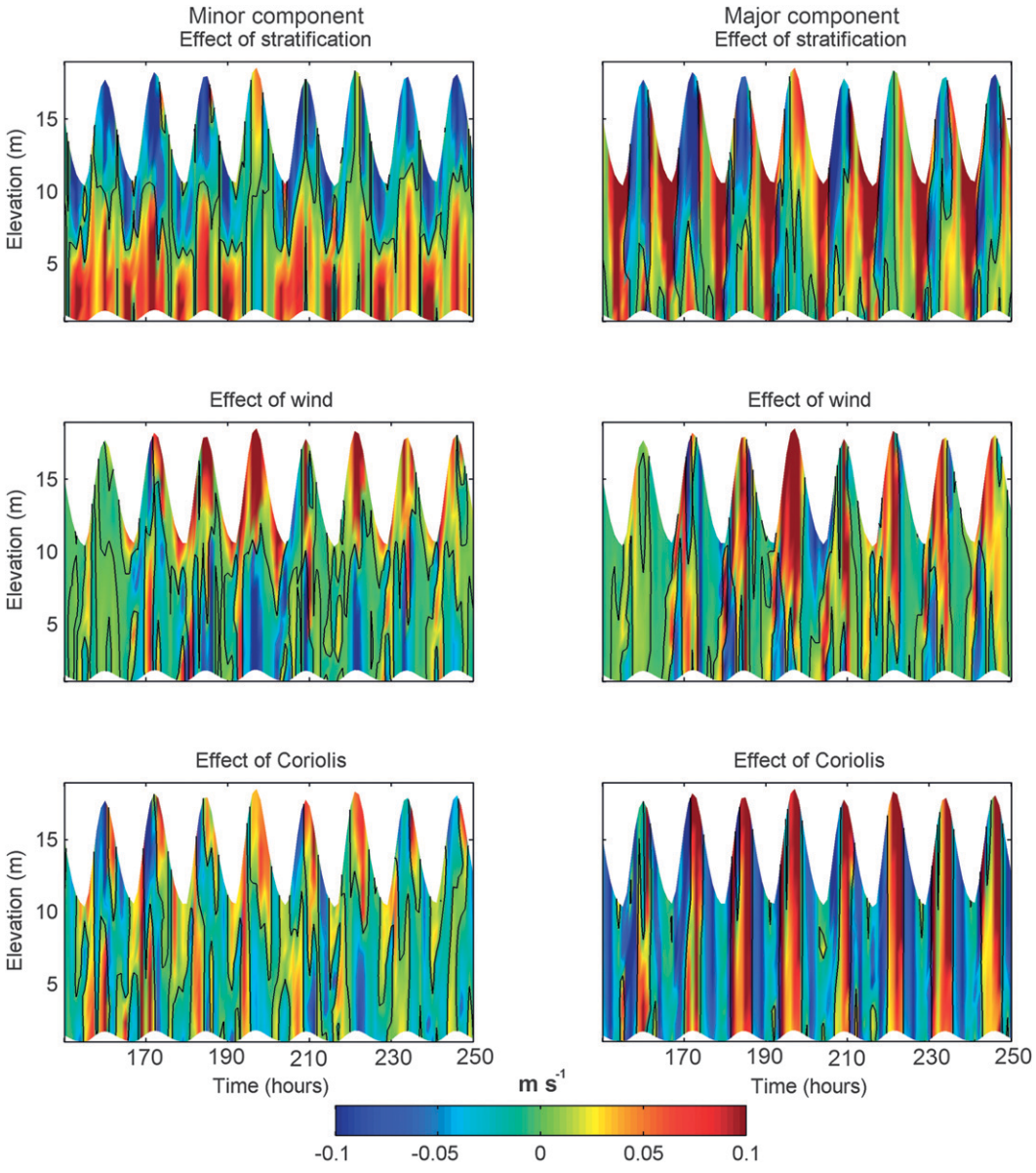

FIG. 13. As in Fig. 12, but for spring tide.

effects to become more important and increased tidal straining enhances the vertical salinity gradients along the channel transporting salty water upstream and fresher water downstream.

6. Conclusions

We investigated the effect of tide, river, wind, and Earth's rotation on the three-dimensional circulation in the Dee, a macrotidal estuary, using a fine-resolution model. At low water, tidal straining and constrained river flow cause stratification. Large spatial variability occurs in the current and residual patterns, with flood-dominated maximum values occurring within the tidal channels.

The two main tidal channels exhibit different behaviors; the Welsh Channel (to the west) is characterized by a horizontal shear in the residual currents and strong tidal influence. Faster tidal velocities and bathymetric steering occur in this channel, producing greater turbulence, mixing, and bottom stress than in the Hilbre Channel. This will also lead to larger resuspension rates, which agree with suspended sediment observation for the same study period (Bolaños et al. 2009). The Hilbre

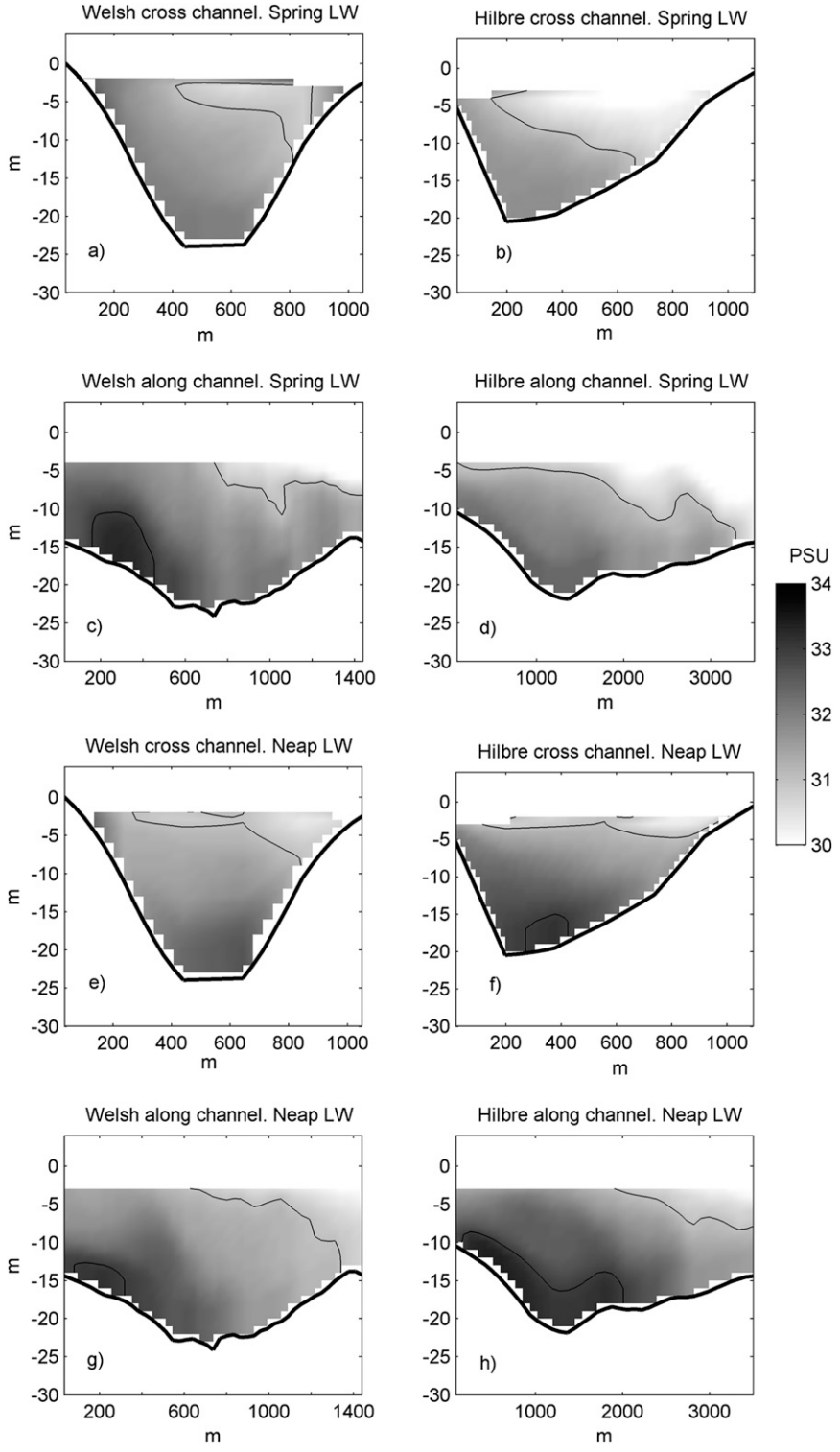

FIG. 14. (a),(b),(e),(f) Across- and (c),(d),(g),(h) along-channels salinity distribution at low water (a),(b),(c),(d) spring and (e),(f),(g),(h) neap for the reference run (P-ref). Salinity contours shown for 31 and 33 PSU.

Channel (to the east) is more strongly influenced by stratification, generating a two-layer system with an offshore surface flow and inward near-bed flow. However, the spatial distribution of the residual current is extremely variable in magnitude and direction.

The time-varying pulses have been analyzed using model simulations. It is shown that the model underestimates stratification and turbulent asymmetry. The turbulence model errors impact the three-dimensional current and density structure, this, together with the bathymetry, are the main sources of uncertainty. Further investigation of different turbulence closures should be performed. Modeled time variation in the residual circulation may therefore be underestimated.

The findings of this work can be summarized as follows.

(i) The model is able to accurately reproduce the minor and major components of depth-averaged velocity when considering river-induced stratification. However, the model fails to reproduce the vertical current structure, producing stronger vertical shear and reduced tidal asymmetry. This is reflected in the vertical profile of residual currents, in which the model reproduces the general pattern of the major component, but not the magnitude. This vertical structure is closely linked to the numerical representation of turbulence, which we believe to be a still imperfect component of the modeling system.

(ii) Scaling law numbers were estimated, showing that they only partially represent the dynamics of the Dee channels. This outlines the importance of 3D unsteady studies and experimental work researching into tidal processes. The importance of the river is underestimated by the use of simplified nondimensional numbers.

(iii) Within the investigated forcing terms the river-induced stratification is dominant in driving the observed residual circulation pattern, even though river flow is relatively small (less than 25 $m^3 s^{-1}$) compared with the tidal fluxes. This demonstrates how important it is to consider river effects (salinity gradients) in a macrotidal estuary even when the interest is at the estuary mouth, away from the river source.

(iv) Wind stress is the second most important forcing, but its influence can vary depending on the specific atmospheric conditions. The tides control the residual circulation by the modulation of stratification through tidal straining, lateral density forcing, and bathymetric river flow constraint. Overall Coriolis has a small contribution but it produces tidal pulses modifying the current and salinity distribution.

(v) In a macrotidal estuary the residual flow pattern is time dependent and the use of tidally averaged quantities may misrepresent any tidal modulation of the baroclinic motions. Tide–stratification–river interaction causes an unsteady pattern of residual circulation and tidal pulses. River-induced pulses are enhanced near low tide accentuating density-driven circulation. At high tide, increased turbulence together with increased estuarine width reduces the river influence and mixes the stratification. The wind also creates pulses in residual flow, stronger near the surface, both at high and low tide. However during low tide the effect is limited to the surface region by stratification.

The physical and morphological characteristics of the Dee Estuary produce a complex circulation. The interaction of the large tidal range, fast tidal currents, river, and wind generate circulation patterns that require three-dimensional studies to properly assess the estuarine dynamics. Thus, for modeling long-term suspended particulate matter and water quality three-dimensional effects and stratification should be included in order to accurately predict the net transport pathways, along with the sediment sources and sinks. Maximum bottom velocities were very similar among the model simulations, thus, sediment resuspension by tidal currents is not strongly affected by these processes, but the resulting long-term transport of the suspension might be. This work demonstrates that even in a macrotidal estuary with weak river flow, time-varying stratification has a major impact on the three-dimensional residual current, and thus, careful model selection (three-dimensional or depth-averaged) should be considered for estuarine studies.

Acknowledgments. This research has been carried out as part of the FORMOST project (NERC Grant NE/E015026/1) and the Ocean 2025 program. Additional support was provided by the EU MICORE (EU FP7 Program Grant 202798) and FIELD-AC (EU FP7 Program Grant 242284) projects. Jane Williams (NOC) is thanked for providing the operational surge model output and meteorological (wind and pressure) data, while Clare O'Neill (NOC, Cobs) is thanked for providing the offshore temperature and salinity fields to the Irish Sea and supplementing the meteorological forcing with air temperature, humidity, and cloud cover to enable full atmospheric forcing. Observations used for model validation were obtained from BODC and the NOC Cobs. Comments from two anonymous reviewers considerably helped to improve this manuscript.

REFERENCES

Bolaños, R., and A. J. Souza, 2010: Measuring hydrodynamics and sediment transport processes in the Dee Estuary. *Earth Syst. Sci. Data,* **2,** 157–165.

——, B. Moate, and A. J. Souza, 2009: Measuring suspended sediment and its wave and turbulence forcing in the Dee estuary. *Impact of Human Activities on Dynamic Coastal Processes,* M. Mizuguchi, and S. Sato, Eds., World Scientific, CD-ROM.

——, L. O. Amoudry, and K. Doyle, 2011: Effects of instrumented bottom tripods on process measurements. *J. Atmos. Oceanic Technol.,* **28,** 827–837.

Brown, J. M., A. J. Souza, and J. Wolf, 2010: An 11-year validation of wave-surge modelling in the Irish Sea, using a nested POLCOMS-WAM modelling system. *Ocean Modell.,* **33,** 118–128.

——, R. Bolanos, and J. Wolf, 2011: Impact assessment of advanced coupling features in a tide-surge-wave model, POLCOMS-WAM, in a shallow water application. *J. Mar. Syst.,* **87,** 13–24.

Burchard, H., 2009: Combined effects of wind, tide and horizontal density gradients on stratification in estuaries and coastal seas. *J. Phys. Oceanogr.,* **39,** 2117–2136.

——, and R. D. Hetland, 2010: Quantifying the contribution of tidal straining and gravitational circulation to residual circulation in periodically stratified tidal estuaries. *J. Phys. Oceanogr.,* **40,** 1243–1262.

Canuto, V. M., A. Howard, Y. Cheng, and M. S. Dubovikov, 2001: Ocean turbulence. Part I: One-point closure model-momentum and heat vertical diffusivities. *J. Phys. Oceanogr.,* **31,** 1413–1426.

Chen, S., and L. P. Sanford, 2009: Axial wind effects on stratification and longitudinal salt transport in an idealized, partially mixed estuary. *J. Phys. Oceanogr.,* **39,** 1905–1920.

Cheng, P., and A. Valle-Levinson, 2009: Influence of lateral advection on residual currents in microtidal estuaries. *J. Phys. Oceanogr.,* **39,** 3177–3190.

——, ——, and H. E. Swart, 2010: Residual currents induced by asymmetric tidal mixing in weakly stratified narrow estuaries. *J. Phys. Oceanogr.,* **40,** 2135–2147.

Fortunato, A. B., A. Oliviera, and A. M. Baptista, 1999: On the effect of tidal flats on the hydrodynamics of the Tagus estuary. *Oceanol. Acta,* **22,** 31–44.

Hansen, D. V., and M. Rattray, 1965: Gravitational circulation in straits and estuaries. *J. Mar. Res.,* **23,** 104–122.

Holt, J. T., and I. D. James, 2001: An S coordinate density evolving model for the northwest European continental shelf. Model description and density structure. *J. Geophys. Res.,* **106** (C7), 14 015–14 034.

Jay, D. A., and J. D. Smith, 1990: Residual circulation in shallow estuaries. 2. Weakly stratified and partially mixed estuaries. *J. Geophys. Res.,* **95** (C1), 733–748.

Kasai, A., A. E. Hill, T. Fujiwara, and J. H. Simpson, 2000: Effect of earth's rotation on the circulation in regions of freshwater influence. *J. Geophys. Res.,* **105** (C7), 16 961–16 969.

Lane, A., 2008: A 3D numerical model of Liverpool Bay for the Coastal Observatory. *Proc. PECS-2008: Physics of Esturies and Coastal Seas,* Liverpool, United Kingdom, Proudman Oceanographic Laboratory, 415–418.

Lerczak, J. A., and W. R. Geyer, 2004: Modeling the lateral circulation in straight, stratified estuaries. *J. Phys. Oceanogr.,* **34,** 1410–1428.

Li, C., and J. O'Donnell, 2005: The effect of channel length on the residual circulation in tidally dominated channels. *J. Phys. Oceanogr.,* **35,** 1826–1840.

MacCready, P., and W. R. Geyer, 2010: Advances in estuarine physics. *Annu. Rev. Mar. Sci.,* **2,** 35–58.

Moore, R. D., J. Wolf, A. J. Souza, and S. S. Flint, 2009: Morphological evolution of the Dee Estuary, Eastern Irish Sea, UK: A tidal asymmetry approach. *Geomorphology,* **103,** 588–596.

Plant, N. G., K. L. Edwards, J. M. Kaihatu, J. Veeramony, L. Hsu, and K. T. Holland, 2009: The effect of bathymetric filtering on near-shore process model results. *Coast. Eng.,* **56,** 484–493.

Prandle, D., 2009: *Estuaries: Dynamics, Mixing, Sedimentation and Morphology.* Cambridge University Press. 236 pp.

Pritchard, D. W., 1952: Salinity distribution and circulation in the Chesapeake Bay estuaries system. *J. Mar. Res.,* **11,** 106–123.

Proctor, R., and I. D. James, 1996: A fine-resolution 3D model of the southern North Sea. *J. Mar. Syst.,* **8,** 131–146.

Schults, E. A., and H. B. Simmons, 1957: Fresh water-salt water density currents, a major cause of siltation in estuaries. U.S. Army Corps of Engineers Committee on Tidal Hydraulics Tech. Bull. 2, 28 pp.

Scully, M. E., C. T. Friedrichs, and J. M. Brubaker, 2005: Control of estuarine stratification and mixing by wind-induced straining of the estuarine density field. *Estuaries,* **28,** 321–326.

Simpson, J. H., J. Brown, J. Matthews, and G. Allen, 1990: Tidal straining, density currents, and stirring in the control of estuarine stratification. *Estuaries,* **13,** 125–132.

Stacey, M. T., 2001: Creation of residual flows in a partially stratified estuary. *J. Geophys. Res.,* **106** (C8), 17 013–17 037.

——, J. P. Fram, and F. K. Chow, 2008: The role of tidally periodic stratification in the creation of estuarine subtidal circulation. *J. Geophys. Res.,* **113,** C08016, doi:10.1029/2007JC004581.

Umlauf, L., H. Burchard, and K. Bolding, 2005: General ocean turbulence model: Source code documentation. Baltic Sea Research Institute Warnemünde Tech. Rep. 63, 346 pp.

Valle-Levinson, A., 2008: Density-driven exchange flow in terms of Kelvin and Ekman numbers. *J. Geophys. Res.,* **113,** C04001, doi:10.1029/2007JC004144.

——, C. Reyes, and R. Sanay, 2003: Effects of bathymetry, friction, and rotation on estuary–ocean exchange. *J. Phys. Oceanogr.,* **33,** 2375–2393.

Wang, B., O. B. Fringer, S. N. Giddings, and D. A. Fong, 2009: High-resolution simulations of a macrotidal estuary using SUNTANS. *Ocean Modell.,* **26,** 60–85.

Williams, J. J., P. S. Bell, L. E. Coates, N. Metje, and R. Selwyn, 2003: Interactions between a benthic tripod and waves on a sandy bed. *Cont. Shelf Res.,* **23,** 355–375.

Winant, C. D., 2008: Three-dimensional residual tidal circulation in an elongated, rotating basin. *J. Phys. Oceanogr.,* **38,** 1278–1295.

Wong, K. C., 1994: On the nature of transverse variability in a coastal plain estuary. *J. Geophys. Res.,* **99** (C7), 14 209–14 222.